16th World Conference on Earthquake, 16WCEE 2017
Santiago Chile, January 9th to 13th 2017
Paper N° 3538
Registration Code: S-I1461879556

IMPORTANCE OF NON-SIMULATED FAILURE MODES IN INCREMENTAL DYNAMIC ANALYSIS (IDA) OF NON-DUCTILE RC FRAMES

B. Alfarah(1), F. López-Almansa(2), S. Oller(3)
(1) *PhD Candidate, Technical University of Catalonia, engbachar@gmail.com*
(2) *Professor, Technical University of Catalonia, francesc.lopez-almansa@upc.edu*
(3) *Professor, Technical University of Madrid, sergio.oller@upc.edu*

Abstract

Nonlinear dynamic analysis of reinforced concrete structures requires a thorough understanding of behavior of structural elements for all levels of performance, especially collapse. Main reason is that reinforced concrete is a mixed material having complicated nonlinear behavior, each element having several coupled degradation modes that influence the entire structure and can change its collapse mechanism. Therefore, using oversimplified models can lead to misleading results. This paper presents a numerical study on the relation among the non-simulated failure modes of the structural elements of non-ductile RC frames and their collapse mechanism; this study reports on the so-called "Structural resurrection" phenomenon in Incremental Dynamic Analysis (IDA). It consists in some structures collapsing under a certain accelerogram, although resisting the same accelerogram but scaled by a factor bigger than unity. This fact was reported, among other examples, in the Van Nuys Hotel; this work focusses on a RC frame of that building. Structural behavior is described with OpenSEES code accounting for flexural, shear and axial failure modes of structural members. Obtained results show that simplified models grossly overestimate the building capacity since several hidden failure modes are only detected by more complex formulations. The so-called structural resurrection might be merely due to the use of too simple models.

Keywords: Structural resurrection, non-ductile RC frames, collapse mechanism, axial failure, shear failure

1. Introduction

Incremental Dynamic Analysis (IDA) [1] consists in determining the dynamic structural response to one or more seismic inputs (accelerograms) scaled with increasing factors. Results are usually represented by the so-called IDA curves. These plots are capacity curves similar to the results of push-over analyses; in the horizontal axis, top level maximum displacement (or other response magnitude with similar meaning) is usually represented, and the vertical axis contains any index related to the excitation severity. Fig. 1 displays example results for Van Nuys Hotel [2] under Imperial Valley (1979, Plaster City record); severity of seismic action is quantified by the spectral response ordinate for the first mode $S_a(T_1, 0.05)$, and the magnitude of the response is quantified by the maximum (along the duration of the earthquake) relative displacement between floors (interstory drift). Fig. 1.a and Fig. 1.b corresponds to accelerograms in different directions. Van Nuys Hotel has a non-ductile RC framed structure and has been considered by the Pacific Earthquake Engineering Research Center (PEER) as a test-bed structure. This construction has been studied by several researchers [3-7] and had been instrumented prior the 1994 Northridge earthquake; therefore, its damage is recorded. Fig. 1.a shows hardening and negative slope of the IDA curve. Fig. 1.b corresponds to structural resurrection, e.g. extreme hardening where not only IDA curve has negative slope but also reaches collapse before recovering. In other cases, structural resurrection is even more obvious, since collapse does not correspond to a single value of input seismic intensity but to a range of values of that parameter [1].

Structural resurrection implies that a given structure collapses under a certain input but is able to resist the same accelerogram scaled with a bigger factor. This circumstance is highly surprising, although conceivable, given the big uncertainties inherent in nonlinear time-history analyses. To investigate completely the feasibility of structural resurrection, it is necessary to account for all the degradation and failure modes and their interaction. For old RC structures, prediction of all collapse mechanisms is more difficult due to the low ductility of the structural elements and the subsequent high possibility to develop uncommon failure modes. In other words, to obtain reliable conclusions, it is necessary to use accurate structural models.

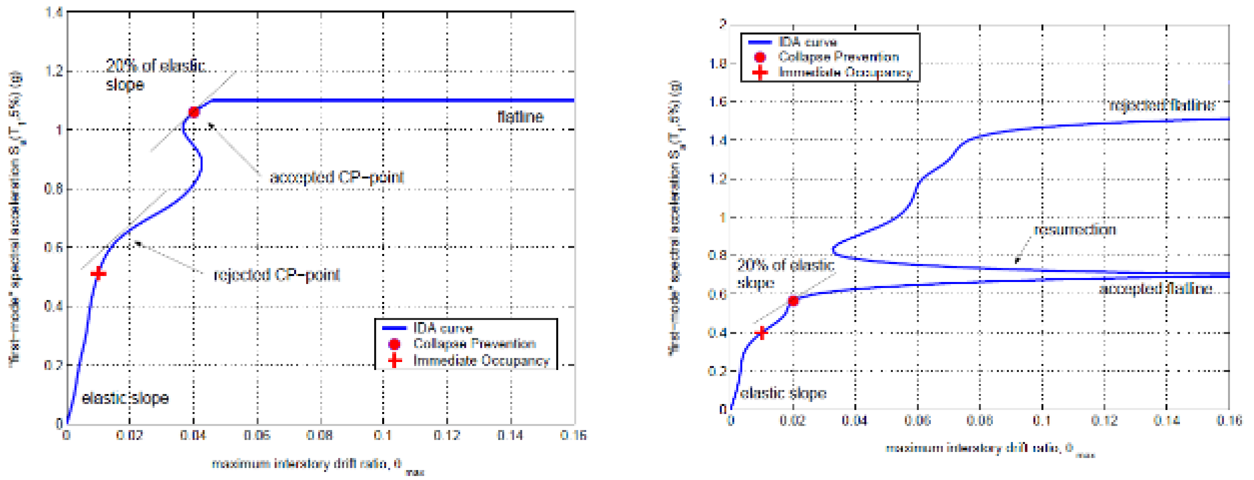

(a) Van Nuys hotel frame. Hardening (b) Van Nuys hotel frame. Structural resurrection

Fig. 1 – Examples of IDA curves [1-2]

Non-simulated degradation modes and their effects on the collapse mechanism have been studied by several researchers. [8] developed fragility functions based on 92 cyclic tests of RC columns; those functions detect column shear failure and subsequent loss of load-carrying capacity by post-processing results from dynamic analysis. Columns yielded first in flexure and then failed in shear, this being the so-called “flexure-shear” failure mode. Aslani defines four damage states: (1) light cracking, (2) severe cracking, (3) shear failure and (4) loss of load-carrying capacity; proposed fragility functions predict the probability of each damage state in terms of drift ratio, axial load ratio and transverse reinforcement amount. [9] carried out IDA analyses for a 8-story RC frame using fragility functions developed by Aslani. Results show that for some records collapse is governed by shear and axial failure modes; for some non-ductile structures, collapse probability increases by 30% after taking into account those modes.

[10] identifies, based on experiments and observations from past earthquakes, main collapse mechanisms of RC frames and element deterioration modes. Collapse mechanisms are classified in vertical and sidesway. Collapse mechanisms and deterioration modes are closely related: flexural hinging leads usually to sidesway collapse, column axial failure leads to vertical collapse, etc.

This paper investigates the importance of the non-simulated failure modes for non-ductile buildings and tries to find a relation with structural resurrection; with this aim, Van Nuys hotel is taken as case study. The structural behavior is described with the finite element code OpenSEES [11]. The drift capacity model developed in [12] is used to capture the shear-axial failure of columns.

2. Building Description

The analyzed building [2] has 7 stories without basements, and its plan configuration is rectangular (63 ft ×150 ft), being uniform along building height. There are 3 bays in one direction and 8 bays in the other direction (Fig. 2 [7]). The long direction is oriented east-west. The building is almost 65 ft tall: the first story is 13 ft, 6 in and stories 2 through 7 are 8 ft, 6 in. The building is a hotel (Van Nuys hotel), being located in San Fernando Valley, California. Was built in 1966. The building experienced several significant earthquakes. Suffered minor structural damage and extensive non-structural damage during 1971 San Fernando earthquake, and extensive structural damage during 1994 Northridge earthquake.

The RC structure has 2-way flat slabs (with beams in the perimeter); inner columns have square cross-section and façade columns have rectangular section. Design was carried out using 1963 version of ACI-318; columns do not have ductile detailing. Strength of columns concrete is f_c' = 5/4/3 ksi for the 1st/2nd and higher stories. Strength of beams and slabs concrete is f_c' = 4 ksi at 1st and 2nd floors and f_c' = 3 ksi at floors 3 to 7. Columns reinforcement is made of A432-62T (Grade 60) steel; beams and slabs reinforcement is ASTM A15-62T and A305-56T (Grade 40). Deeper description of the structure can be found in [7].

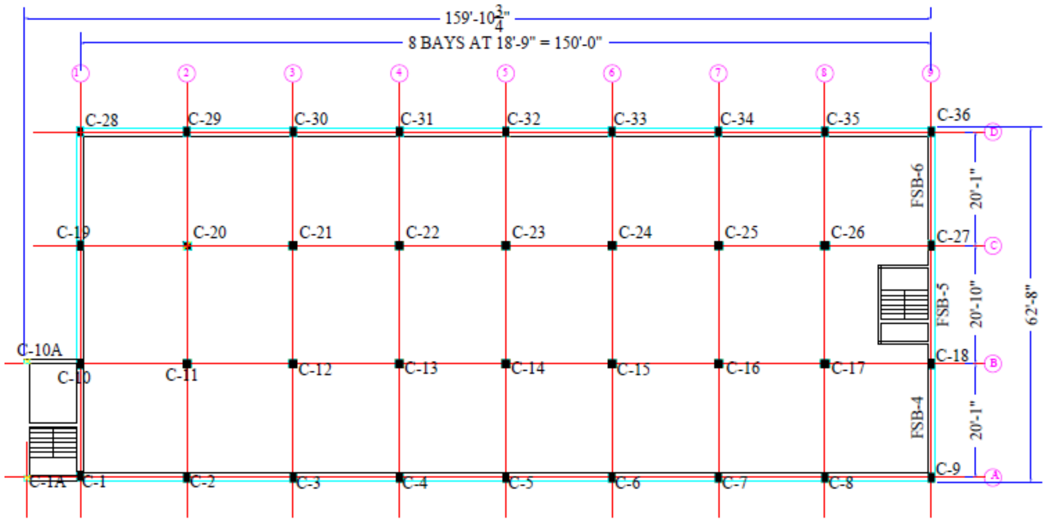

Fig. 2 – Structural plan of Van Nuys Hotel [7]

In this work, the seismic performance of the building is analyzed in the short direction. The structure is represented by a 2-D façade frame, corresponding to axis (9) in Fig. 2.

3. Analytical Models of the Van Nuys Hotel Frame

3.1 General

As discussed previously, the performance of the building in its short direction is studied by analyzing a single planar frame, see Fig. 3. To estimate the contribution of this frame to the initial lateral stiffness of the building, a linear 3D model of the whole structure is built using SAP 2000 [13]. Obtained percentage is 18%; the building mass is assigned accordingly. Seismic weight corresponds to $D + 0.3\,L$. Additional loads are applied at column ends to better represent the actual observed 3-D behavior.

The nonlinear static and dynamic behavior of the analyzed frame is simulated with OpenSEES code [11]. Frame elements are discretized with Navier-Bernouilli beam-column elements. Additional joints are used to account for the higher stiffness of the intersection between columns and beams (Fig. 3.c). Second order effects are accounted for by a P-delta analysis. The consideration of nonlinear behavior in columns and beams is described next.

Columns. Nonlinear behavior is modelled with distributed plasticity using fiber models and Gauss–Lobatto quadrature rule using the Force-Based formulation with five integration points. Concrete uniaxial behavior is represented with material model “Concrete01”, with zero tensile strength and a parabolic stress-strain law in compression followed by a linear descending branch. Concrete confinement is taken into consideration. Behavior of reinforcement bars is simulated with “Steel 02” material model.

Beams. Lumped plasticity models with rotational springs are used (Fig. 3.b). This more simplified formulation is considered because beams were only slightly damaged in both San Fernando and Northridge events [6]. Moment- curvature laws are bilinear; parameters are obtained after program XTRACT [14]. The effective flexural stiffness is estimated as 0.35 EI_g in the first, sixth and seventh floors and 0.4 EI_g for all the other floors; these coefficients are selected according to the sectional parameters.

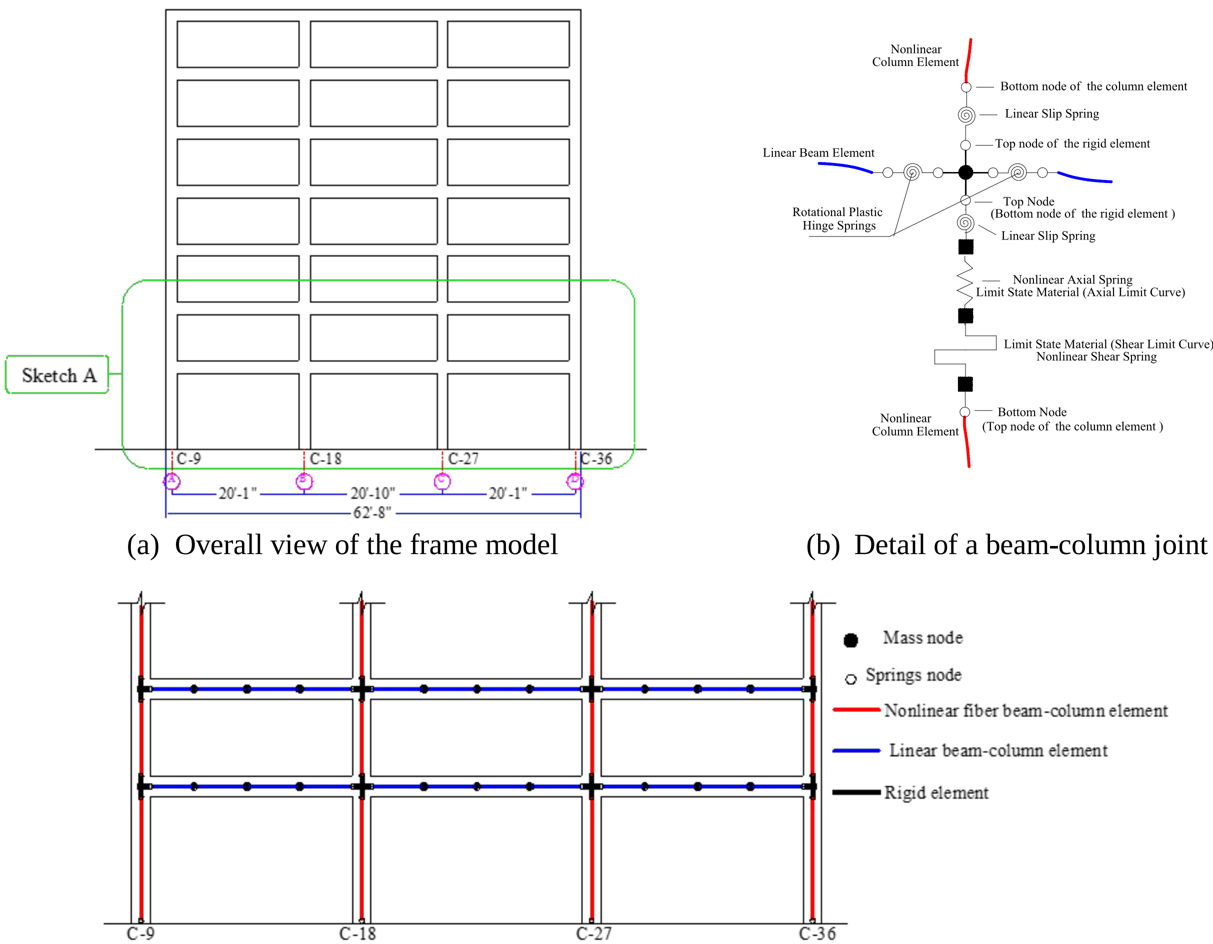

(a) Overall view of the frame model

(b) Detail of a beam-column joint

(c) Zoomed view of the model

Fig. 3 – Model of the Van Nuys Hotel Frame

3.2 Bond-slip effects

The effect of longitudinal reinforcement slip at column ends is represented by an increase in rotation angle. This effect is simulated by zero-length linear rotational springs, as shown in Fig. 3.b. Stiffness of springs is selected as recommended by [15]:

$$K_{\text{slip}} = \frac{8\, f_{\text{b}}}{d_{\text{b}}\, f_{\text{s}}}\, EI_{\text{flex}} \tag{1}$$

In equation (1), d_b is the bar nominal diameter, EI_{flex} is the column effective flexural rigidity at first yield, f_s can be taken equal to yield stress f_{y} [16], and f_{b} is the bond stress $0.8\sqrt{f'_{\text{c}}}$ (MPa) [17].

3.3 Column shear-axial failure model

Shear failure of columns of Van Nuys hotel has been studied by several researchers using diverse failure models. [2] used two types of non-interacting springs: translation spring in the middle section and two rotation springs at column ends to model shear and flexure degradation, respectively. Krawinkler [7] used shear force versus shear distortion model. Krawinkler model is independent on load history and drift demand; initial shear strength is selected according to [18] assuming that concrete contributes only to the minimum residual capacity and post-peak response is modelled as highly brittle.

Several studies [19-21] have shown that shear strength decays with increased inelastic deformation; in other words, shear failure model should be based on both force and deformation. For this reason, in this work axial and shear limit curves [12] are generated using axial and shear springs that are series connected with the nonlinear fiber column elements, Fig. 3.b.

Shear spring predicts failure according to an empirical drift function [22] based on experimental results; later, axial failure results from sliding along a critical inclined shear crack. Next equations provide drift angle at shear failure (Δ_s / L) and at axial failure (Δ_a / L) (L is column length):

$$\frac{\Delta_s}{L} = \frac{3}{100} + 4\,\rho'' - \frac{1}{40}\frac{\nu}{\sqrt{f'_c}} - \frac{1}{40}\frac{P}{A_g f'_c} \geq \frac{1}{100} \qquad \frac{\Delta_a}{L} = \frac{4}{100}\frac{1+\tan^2\theta}{\tan\theta + P\dfrac{S}{A_{st}\,f_{yt}\,d_c\tan\theta}} \tag{2}$$

In equations (2), ρ” is transverse reinforcement amount, ν is shear stress ratio (demand / capacity), P / $A_g\ f'_c$ is axial load ratio, d_c is column core depth between centre lines of stirrups, S is transverse reinforcement spacing, A_{st} and f_{yt} are area and yield point of transverse reinforcement, and θ is critical crack angle (θ = 65º, [22]). Units are in MPa.

3.4 Effective lateral stiffness of columns

The objective of this subsection is to obtain the effective lateral stiffness of columns (EI_{eff}). It influences behavior after shear failure. When the response reaches the shear limit curve (Δ_s / L in equation (2)), the backbone curve of the shear spring is redefined, as shown in Fig. 4.a. The degraded stiffness K_{deg} can be calculated by assuming that axial failure occurs when the shear strength degrades almost to zero [23], by using the calculated drift at axial failure as presented in Fig. 4.b.

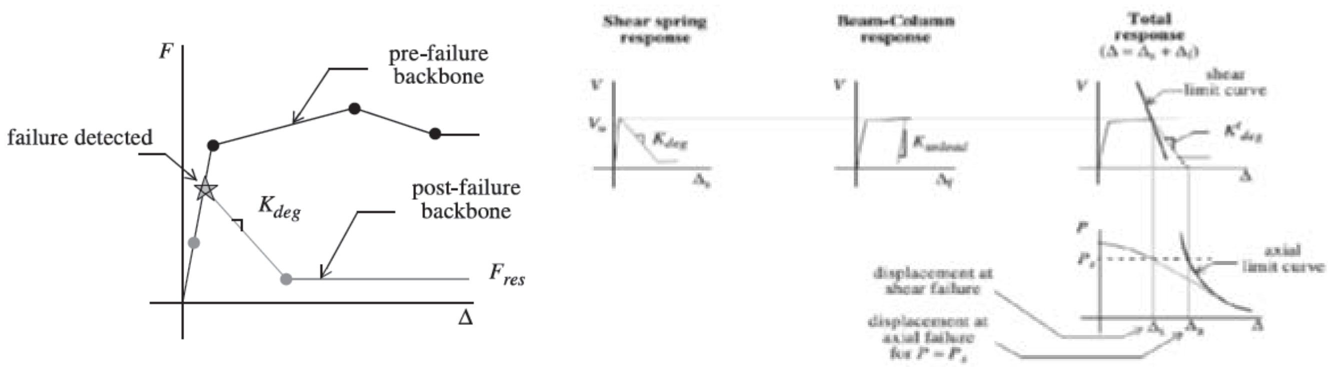

(a) Backbone curve of shear spring after failure

(b) Determination of the degraded stiffness

Fig. 4 – Determination of the degraded stiffness K_{deg} [12]

The total degraded stiffness K^t_{deg} (Fig. 4.b) can be estimated as the following kinematic expression:

$$K^t_{deg} = \frac{V_u}{\Delta_a - \Delta_s} \tag{3}$$

In equation (3), V_u is the column shear capacity. Since beam column element and shear spring are series connected, shear degraded stiffness can be calculated from

$$\frac{1}{K_{deg}} = \frac{1}{K^t_{deg}} - \frac{1}{K_{unload}} \tag{4}$$

In equation (4), K_{unload} is the column unloading flexural stiffness given by 12 EI_{eff} / L^3, where EI_{eff} is the effective bending stiffness of column. In [24], it is taken as 0.7 E_cI_g or 0.5 E_cI_g depending on if compression due to gravity loads is > 0.5 A_gf_c’ or < 0.3 $A_gf'_c$, respectively. Instead of this simplified approach, in this research a more accurate method to calculate the effective bending stiffness of column is used; this formulation is based on obtaining yield column displacement (Δ_y). Δ_y can be estimated as the sum of displacements due to flexural, slip and shear effects:

$$\Delta_{\mathrm{y}} = \Delta_{\mathrm{flex}} + \Delta_{\mathrm{slip}} + \Delta_{\mathrm{shear}} \tag{5}$$

Flexural, slip and shear displacements can be estimated [25] as:

$$\Delta_{\mathrm{flex}} = \frac{L^2}{6}\,\phi_{\mathrm{y}} = \frac{L^2}{6}\,\frac{M_{\mathrm{SP}}}{EI_{\mathrm{flex}}} \qquad \Delta_{\mathrm{slip}} = \frac{L\, d_{\mathrm{b}}\, f_{\mathrm{s}}\, \phi_y}{8\, f_{\mathrm{b}}} \qquad \Delta_{\mathrm{shear}} = \frac{2\, M_{\mathrm{SP}}}{GA_{\mathrm{eff}}} \tag{6}$$

In equation (6), ϕ_{y} is yield curvature, M_{SP} is moment at spalling of concrete, EI_{flex} is effective flexural stiffness, and GA_{eff} is effective shear stiffness. Flexural displacement is obtained assuming that column is clamped at both ends and that curvature varies linearly along height. M_{SP} corresponds to concrete strain 0.005. EI_{flex} can be determined from the moment and curvature at first yield. Finally, EI_{eff} can be obtained from:

$$EI_{\mathrm{eff}} = \frac{L^2}{6}\,\frac{M_{\mathrm{SP}}}{\Delta_{\mathrm{y}}} \tag{7}$$

3.5 Models considered in the analysis

To highlight the importance of shear-axial failure of columns followed by a loss of their bearing capacity, four models are used in the analysis:

1. **First model**. Corresponds to the simple models that are most commonly used in earthquake engineering. Can simulate the material degradation through the constitutive models. Second-order effects are accounted for. This model is able to simulate only the sidesway collapse mechanism due to flexural degradation.
2. **Second model**. Like first model although without second-order analysis.
3. **Third model**. This model is similar to first one, but considers also shear failure by attaching a shear failure spring in series with a bond slip element at each column top.
4. **Fourth model**. This model is generated after third one. The most critical columns in terms of potential axial failure are identified; in those that have experienced shear failure, axial limit spring is attached. Post-processing is necessary to check if there are other columns having reached their axial limit curve. This model is able to predict sidesway and vertical collapse mechanisms. Noticeably, progressive collapse is detected.

4. Pushover Analysis

Nonlinear static (pushover) analyses are carried out; pushing forces vary along building height as first modal shape. Fig. 5 and Fig. 6 display, for each model, capacity curve and final state, respectively.

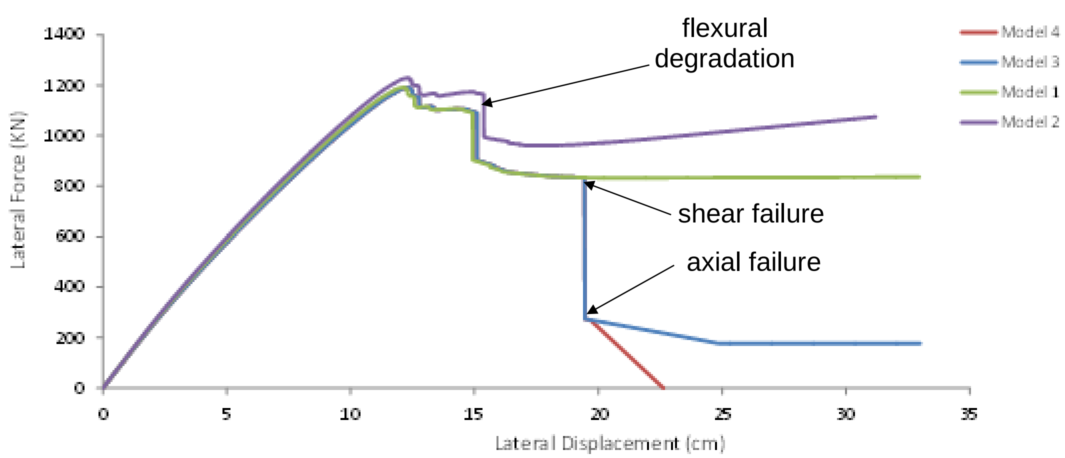

Fig. 5 – Capacity curve of the frame (four models)

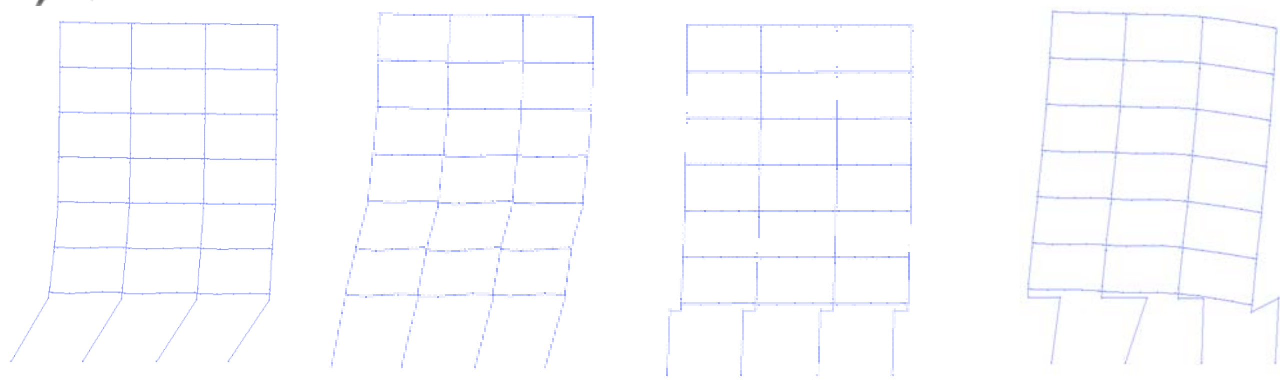

(a) Model 1 (b) Model 2 (c) Model 3 (d) Model 4

Fig. 6 – Deformation at collapse for each model

Fig. 5 shows that the four models predict almost same behavior before reaching the maximum force capacity. After that point, all models describe flexural degradation. Difference between first and second models can be explained by influence of second-order effects; noticeably, both models provide highly ductile responses. Until shear failure is detected, third and fourth models deliver similar results than first one; in that moment, a brittle vertically descending branch is generated. Then, after reaching the residual strength, axial failure is detected by the fourth model; a linear descending branch (negative slope) follows that point. As expected, Fig. 5 shows that, the more failure modes are accounted for, the less capacity is predicted. Therefore, using over-simplified models leads to significant unconservative errors. Fig. 6.c shows that shear failure arose in first floor columns, thus being a brittle collapse mechanism.

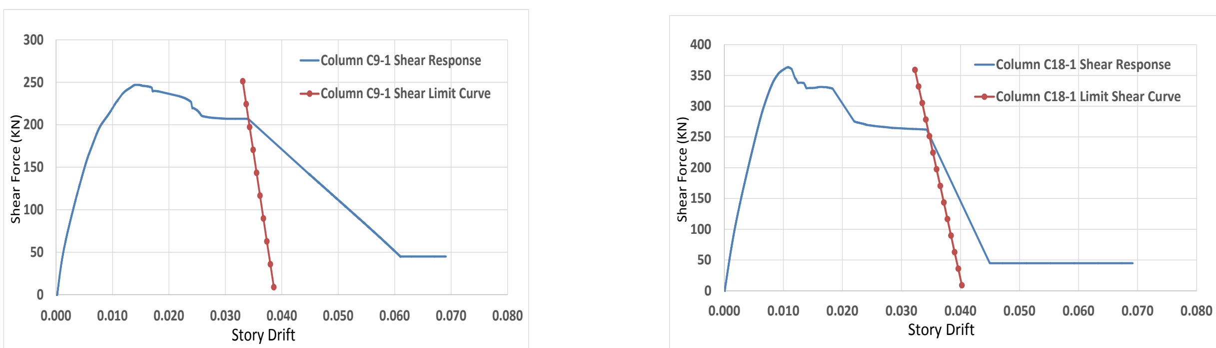

(a) Column C9-1 (left) (b) Column C18-1 (second)

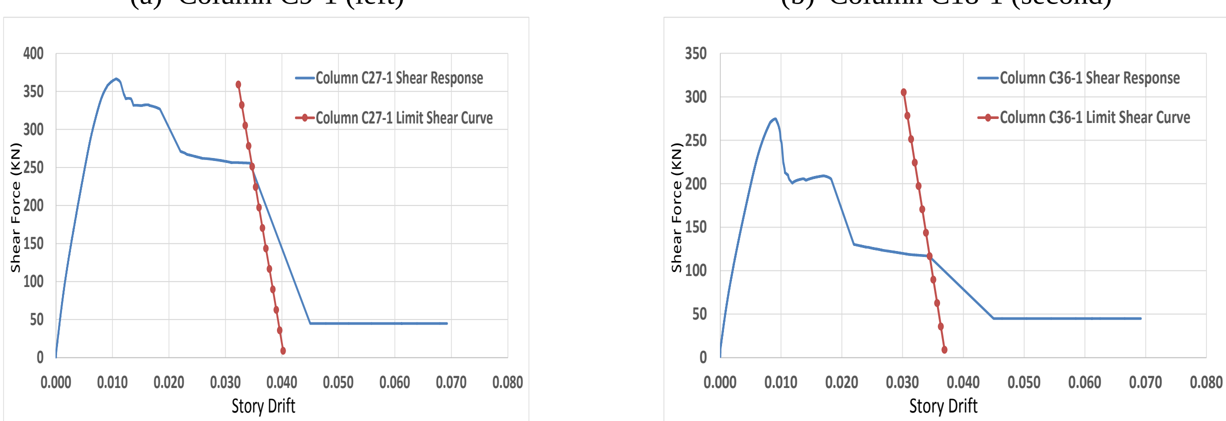

(c) Column C27-1 (third) (d) Column C36-1 (right)

Fig. 7 – First floor columns shear force vs. story drift. Model 3

Fig. 7 displays, from model 3, shear force vs. drift plots for first floor columns (C9-1, C18-1, C27-1 and C36-1, Fig. 2 and Fig. 3). Fig. 8 displays plots of shear force in each first floor column vs. top floor displacement. Fig. 7 shows that, after reaching the limit curve (Δ_s / L in equation (2)), shear response degrades with the total degraded stiffness K^t_{deg} (equation (3)), until reaching a defined residual shear force. Fig. 7 and Fig. 8 show that, as expected, early failure appears in the most loaded column (C36-1, right).

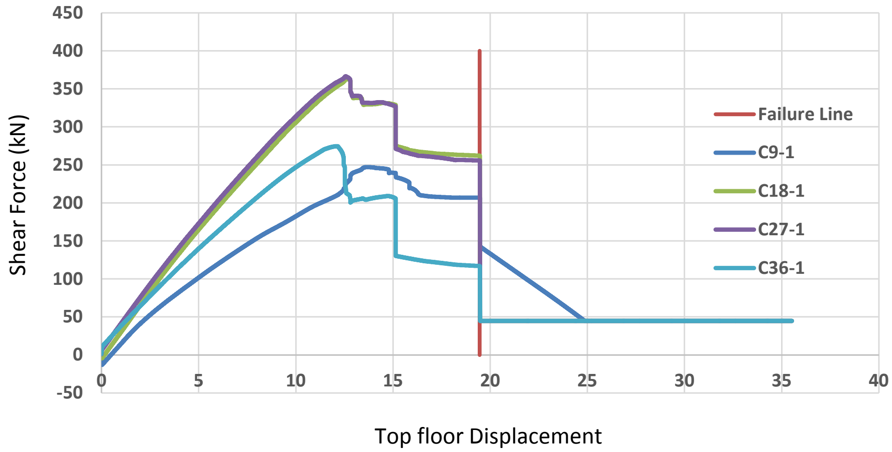

Fig. 8 – First floor columns shear force vs. top floor displacement. Model 3

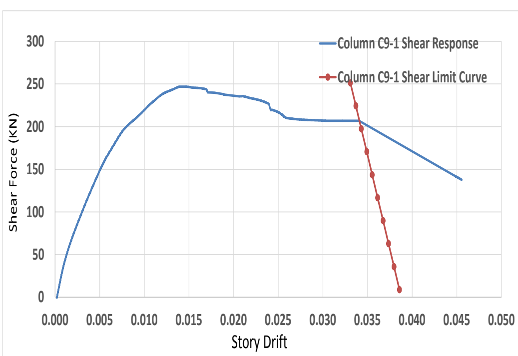

(a) Column C9-1 (left)

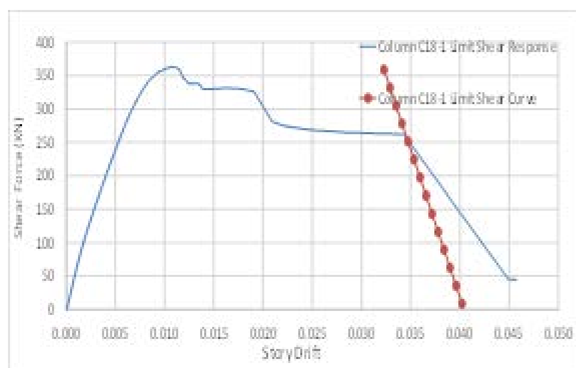

(b) Column C18-1 (second)

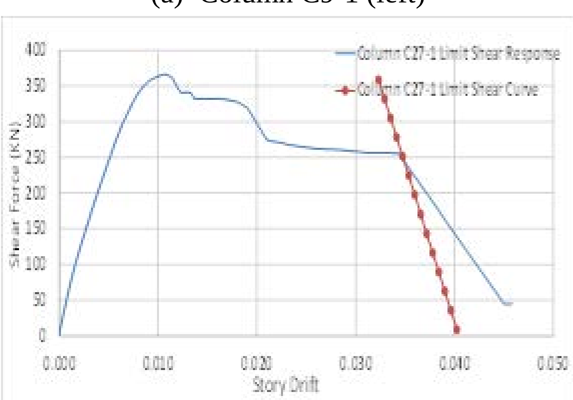

(c) Column C27-1 (third)

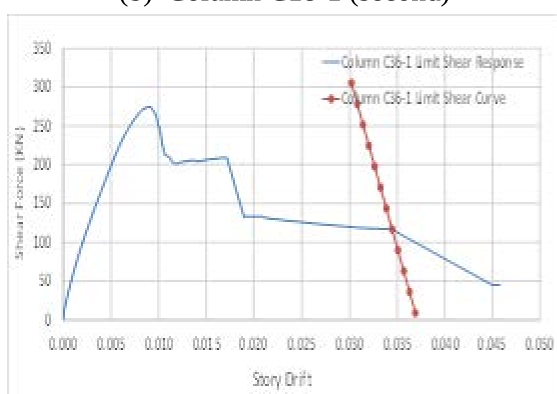

(d) Column C36-1 (right)

Fig. 9 – First floor columns shear force vs. story drift. Model 4

Fig. 9 displays analogous plots than Fig. 7, although from model 4. Results from both models are alike until the axial limit curve is reached, then a sudden failure is detected by model 4. This circumstance can be observed in Fig. 10, displaying plots of axial force vs. story drift for the most loaded column (C36-1, right). After failure of column C36-1 (Δ_a / L in equation (2)), its bearing capacity is lost, the load is transferred to other columns, thus generating a vertical collapse mechanism as shown in Fig. 6.d.

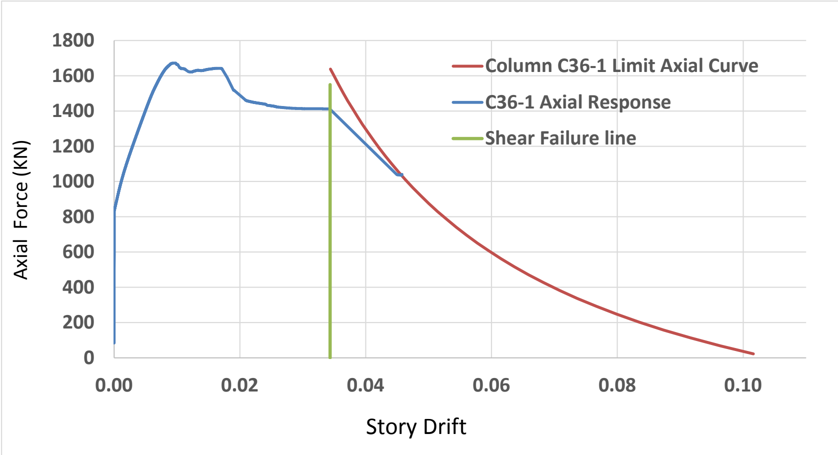

Fig. 10 – Axial force vs. drift. Column C36-1. Model 4

This analysis matches the observed damage from 1994 Northridge earthquake. Damage was most severe in the south longitudinal perimeter frame, and five out of nine columns between 4th and 5th floors failed in shear [26]. There was column and joint shear damage at 18 different locations. Fig. 11 displays a column that failed in shear [27]. These failures were so serious that some researchers believe that the building could have collapsed if the duration of the strong motion had been greater [28].

(a) Outside view

(b) Inside view

Fig. 11 – Column shear failure of Van Nuys Hotel frame, 1994 Northridge earthquake [27]

5. Nonlinear Dynamic Analysis

Incremental Dynamic Analysis (IDA) is carried out for one record of 1979 Imperial Valley ground motion, Plaster City station with PGA 0.042 g. Noticeably, this input was also considered for IDA analysis displayed in Fig. 1.d. Models 1 and 4 are considered. In model 1, stiffness and mass-proportional Rayleigh damping is used; damping ratio is 5% at first and second modes. In model 4, just mass-proportional damping (5%) is used; stiffness-proportional damping cannot be used due to unrealistically large damping forces resulted from sudden shear and axial failure of zero-length springs [25].

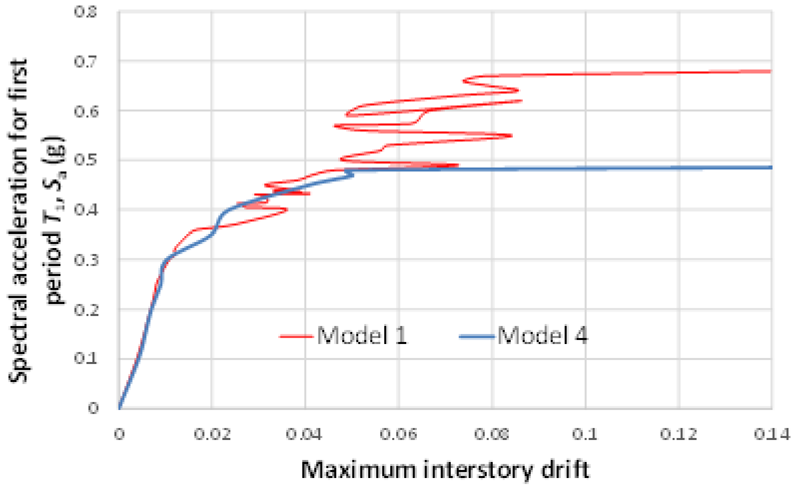

Fig. 12 – IDA curves. Imperial Valley ground motion

Fig. 12 displays IDA curves in terms of maximum interstory drift vs. spectral acceleration at the building fundamental period ($S_a(T_1)$). Comparison between curves for model 1 and 4 shows that the use of oversimplified models grossly overestimates the seismic capacity. Fig. 12 shows that model 1 predicts negative slope before reaching collapse at S_a = 0.68 g. Comparison with the IDA curves in Fig. 1.d shows big similarity, apart from the structural resurrection. Model 4 provides a smoother behavior, with collapse at S_a = 0.49 g; it arises by shear-axial failure of first floor columns and loss of axial carrying capacity of columns C9-1, C18-1 and C27-1. Fig. 13 presents four consecutive states of this brittle progressive collapse. State 1 (Fig. 13.a) corresponds to shear failure of left column (C9-1). State 2 (Fig. 13.b) corresponds to shear failure of inner columns (C18-1 and C27-1). State 3 (Fig. 13.c) corresponds to loss of axial carrying capacity of left column (C9-1). In state 4 (Fig. 13.d), inner columns (C18-1 and C27-1) also lose their bearing capacity. Fig. 14 displays, similarly to Fig. 10, plots of axial force vs. story drift for first floor columns. Fig. 14 confirms that columns C9-1, C18-1 and C27-1 reach

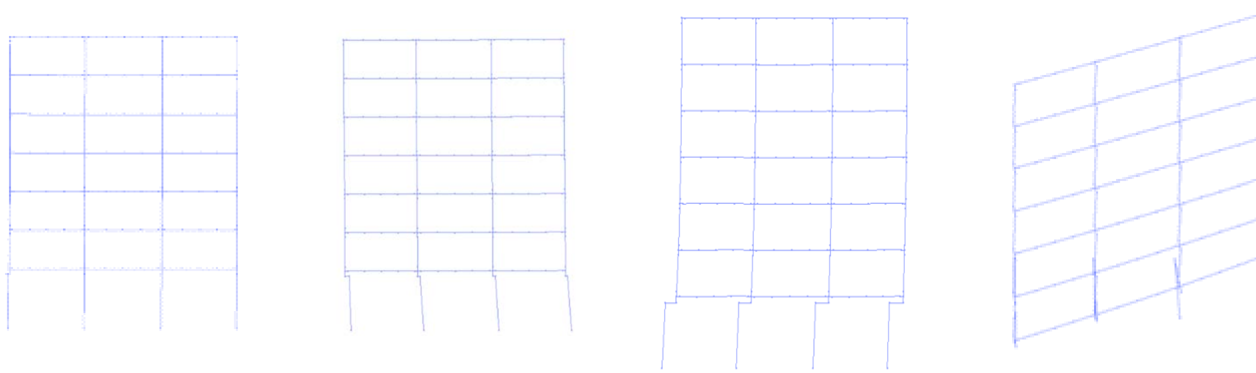

(a) State 1 (b) State 2 (c) State 3 (d) State 4

Fig. 13 – Failure states. Imperial Valley ground motion. Model 4

their axial limit curves; bigger losses are experienced by columns C9-1 (mainly) and C18-1.

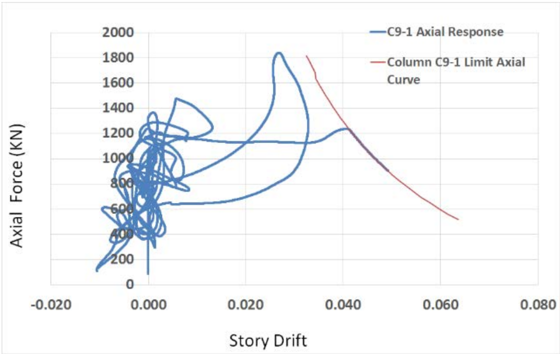

(a) Column C9-1 (left)

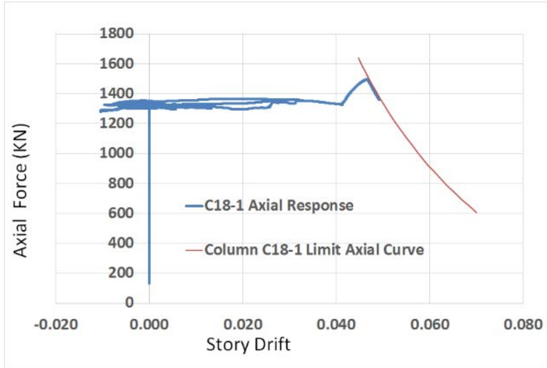

(b) Column C18-1 (second)

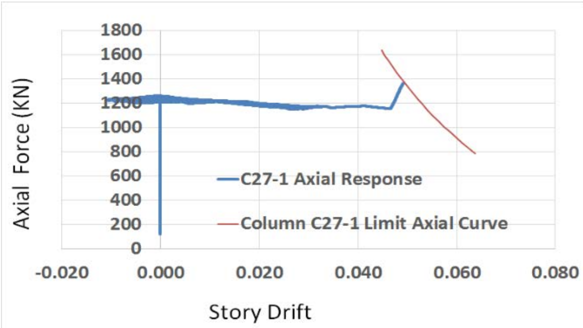

(c) Column C27-1 (third)

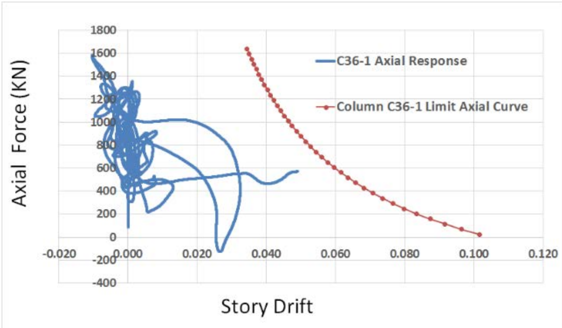

(d) Column C36-1 (right)

Fig. 14 – Axial response of first floor columns vs. drift. Imperial Valley ground motion. Model 4

6. Conclusions

This paper presents a numerical study of the seismic capacity of a non-ductile RC building. The nonlinear structural behavior is described with four models; the most simplified considers only flexure failure while the most accurate considers also shear and axial failure of columns. Pushover and IDA analyses are carried out. Obtained results show that the simplified models grossly overestimate the building capacity. The most accurate model captures all the failure modes and the collapse mechanisms.

The main conclusion of this work is that using over-simplified models can lead to significant unconservative errors. Comparison with previous studies shows that the so-called structural resurrection might be merely due to the use of too simple models.

7. Acknowledgements

This work has received financial support from Spanish Government under projects BIA2014-60093-R and CGL2015-6591. These supports are gratefully acknowledged.

8. References

[1] Vamvatsikos D, Cornell CA (2002): Incremental dynamic analysis. *Earthquake Engineering & Structural Dynamics*, **31** 491-514. DOI: 10.1002/eqe.141.

[2] Vamvatsikos D, Jalayer F, Cornell CA (2003): Application of Incremental Dynamic Analysis to an RC-Structure. FIB Symposium on Concrete Structures in Seismic Regions, Athens.

[3] Jennings PC (1971): Engineering Features of the San Fernando Earthquake of February 9, 1971. *Report EERL 71–02*, California Institute of Technology.

[4] Scholl RE, Kustu O, Perry CL, Zanetti JM (1982): Seismic Damage Assessment for High-Rise Buildings. *Report URS/JAB 8020*, URS/John A. Blume & Associates, San Francisco.

[5] Islam MS (1996a): Analysis of the Northridge Earthquake Response of a Damaged Nonductile Concrete Frame Building. *The Structural Design of Tall Buildings*, **5** 151-182.

[6] Trifunac MD, Ivanovic SS, Todorovska MI (1999): Instrumented 7-Storey Reinforced Concrete Building in Van Nuys, California: Description of the Damage from the 1994 Northridge Earthquake and Strong Motion Data. *Technical Report CE 99-02*, University of Southern California.

[7] Krawinkler H (2005): Van Nuys Hotel Building Testbed Report: Exercising Seismic Performance Assessment, *Technical Report 2005/11*, Pacific Earthquake Engineering Research Center.

[8] Aslani H (2005): Probabilistic Earthquake Loss Estimation and Loss Disaggregation in Buildings. *Doctoral Dissertation*, Stanford University.

[9] Liel AB (2008): Assessing the Collapse Risk of California's Existing Reinforced Concrete Frame Structures: Metrics for Seismic Safety Decisions. *Doctoral Dissertation*, Stanford University.

[10] FEMA P695 (2009): *Quantification of Building Seismic Performance Factors*, Federal Emergency Management Agency.

[11] McKenna F, Fenves GL, Scott MH, Jeremic B (2000): Open System for Earthquake Engineering Simulation (OpenSees). *Pacific Earthquake Engineering Research Center*, Berkeley.

[12] Elwood KJ (2004): Modelling failures in existing reinforced concrete columns. *Doctoral Dissertation*, University of British Columbia.

[13] Computers & Structures Inc. (2015): CSI Analysis Reference Manual for SAP2000®, ETABS®, and SAFE™, available from www.comp-engineering.com.

[14] Imbsen CC (2002): XTRACT Software. Cross-Section Analysis Program for Structural Engineers. 2.6.2 *Imbsen and associates, Inc*.

[15] Elwood KJ, Eberhard MO (2009): Effective Stiffness of Reinforced Concrete Columns. *ACI Structural Journal*, **106**(4) 476-484.

[16] Berry M, Parrish M, Eberhard M (2004): PEER Structural Performance Database User's Manual, (www.ce.washington.edu/~peera1), Pacific Earthquake Engineering Research Center.

[17] Yavari S, Lin SH, Elwood KJ (2008): Study on collapse of flexure-shear-critical reinforced concrete frames. 14th World Conference on Earthquake Engineering, Beijing, China.

[18] Kowalsky MJ, Priestley MJN (2000): Improved analytical model for shear strength of circular reinforced concrete columns in seismic regions. *ACI Structural Journal*, **97**(3) 388-396.

[19] Watanabe F, Ichinose T (1992): Strength and ductility of RC members subjected to combined bending and shear. *Concrete shear in earthquake*. Elsevier 429–438.

[20] Priestley MJN, Verma R, Xiao Y (1994): Seismic shear strength of reinforced concrete columns. *Journal of Structural Engineering*, **120**(8) 2310–2329.

[21] Sezen H (2002): Seismic response and modeling of reinforced concrete building columns. *Doctoral Dissertation*, University of California Berkeley.

[22] Elwood KJ, Moehle JP (2003): Shake Table Tests and Analytical Studies on the Gravity Load Collapse of Reinforced Concrete Frames. *PEER Report 2003/01*. Pacific Earthquake Engineering Research Center.

[23] Nakamura T, Yoshimura M (2002): Gravity load collapse of reinforced concrete columns with brittle failure modes. *Journal of Asian Architecture and Building Engineering*, **1**(1): 21–27.

[24] FEMA 356 (2000): *Prestandard and Commentary for the Seismic Rehabilitation of Buildings*, Federal Emergency Management Agency.

[25] Elwood KJ, Moehle JP (2006): Idealized Backbone Model for Existing Reinforced Concrete Columns and Comparisons With FEMA 356 Criteria. *The Structural Design of Tall and Special Buildings* **15** 553–569. DOI: 10.1002/tal.382.

[26] Gilmartin UM, Freeman SA, Rihal SS (1998): Using earthquake strong motion records to assess the structural and nonstructural response of the 7-story van Nuys hotel to the Northridge earthquake of January 17, 1994, 6th National Conference on Earthquake Engineering, Seattle.

[27] Naeim F (1997): Performance of extensively instrumented building during the January 17, 1994 Northridge earthquake. *California Strong Motion Instrumentation Program*.

[28] Islam MS (1996b): Holiday Inn, 1994 Northridge Earthquake Buildings Case Study Project Proposition 122: Product 3.2, Seismic Safety Commission, 189-233.